

Control of a Transfemoral Prosthesis on Sloped Terrain using Continuous and Nonlinear Impedance Parameters

Namita Anil Kumar¹, Woolim Hong¹, and Pilwon Hur²

Abstract—The design of impedance controllers for sloped walking with a transfemoral prosthesis is a complex control problem that generally results in numerous tuning parameters. This study proposes an easy-to-tune sloped walking control scheme. While the ankle is controlled using impedance control, the knee is controlled using a hybrid strategy of impedance control and trajectory tracking. This study derived continuous, nonlinear impedance functions for the ankle and knee joints using optimization. Principal component analysis of the impedance functions revealed trends that can be used to design impedance controllers for any given slope angle. Said trends were further used to establish a tuning regime which was subsequently tested on a transfemoral prosthesis in an emulator study. The generated gait kinematics and kinetics were found to follow the trends of healthy sloped walking data.

I. INTRODUCTION

Walking is crucial to our existence, yet many individuals with lower-limb disabilities cannot do so. About 185,000 lower-limb amputations are performed annually [1], [2], with amputees suffering from severe decrease in quality of life [3]. Current methods of restoring mobility are also sub-par when compared with healthy human walking. Specifically, many results involve using passive devices such as passive orthoses, stumps, and micro-processor knees. However, passive devices fail to emulate many aspects of healthy human walking such as gait symmetry. On the other hand, powered lower-limb prostheses and exoskeletons hold much more promise in emulating healthy human walking, specifically by allowing for a greater range of motion and propulsion [4], [5]. Unfortunately, most powered devices cannot handle all types of terrain, such as changes in slope. This presents itself as a complex controls problem since human gait kinematics and kinetics vary with the terrain's slope [6]–[11]. Some have proposed Hybrid Zero Dynamics [12], [13], but this may compromise user comfort [14]. An alternative control strategy called Impedance Control offers more user comfort, but involves far too many tuning parameters [15]–[18]. These shortcomings limit the scope of powered prostheses for public usage. The aim of this paper is to develop an intuitive impedance controller with a relatively easier tuning protocol.

*This work was not supported by any organization (Corresponding author: Pilwon Hur)

¹Namita Anil Kumar and Woolim Hong are with the department of Mechanical Engineering, Texas A&M University, College Station, TX 77843, USA Email: namita.anilkumar@tamu.edu, ulim8819@tamu.edu

²Pilwon Hur is with the School of Mechanical Engineering, Gwangju Institute of Science and Technology, Gwangju 61005, South Korea. He is also affiliated with the Department of Mechanical Engineering, Texas A&M University, College Station, TX 77843, USA Email: pilwonhur@gist.ac.kr, pilwonhur@tamu.edu

A. Impedance control of powered prostheses

A popular strategy is impedance control, where the control input to the joint is characterized by the following equation.

$$\tau = K(\theta - \theta_{eq}) + D\dot{\theta} \quad (1)$$

The terms K and D represent the stiffness and damping of the joint, while θ and $\dot{\theta}$ signify the angular position and velocity of the joint. θ_{eq} is the equilibrium angle of the joint. The collection of K , D , and θ_{eq} can be referred to as impedance parameters. Most studies employ a finite state machine, wherein the gait cycle (one heel-strike to another on the same limb) is sectioned into 4-6 stages. Impedance control strategies assign a set of impedance parameters (K, D, θ_{eq}) for each stage of the finite state machine. In [15], these parameters were enforced to be scalars. The parameters were estimated using a least squares method. These estimates were tuned for each slope angle and implemented on a transfemoral prosthesis for up-slope walking. This approach has two challenges: (i) The sectioning of the gait cycle would have to change based on the slope angle. Any mistimed gait sections, particularly during swing phase, could lead to stumbles or falls. (ii) For each gait section, one must tune three impedance parameters per joint—resulting in 24-36 tuning parameters.

B. Improving impedance control for sloped walking

To overcome the above shortcomings, [11] proposed a hybrid controller composed of impedance control during the stance phase and trajectory tracking during the swing phase. This eliminates the issue of mistimed gait sections and considerably reduces the number of tuning parameters in the swing phase. In [11], the impedance parameters K and D linearly increased during the stance phase, but this linear trend did not vary across the different slope angles.

Since human joint angles and torques are continuous in nature, it may be reasonable to enforce similar trends in joint impedances to ensure human-like qualities. Perturbation studies on healthy human walking [19]–[21] found that the ankle's stiffness and damping varied in a nonlinear continuous fashion across the gait cycle. Further, it is advantageous to design controllers with continuous control input to avoid jerk. While studies such as [18], [22], [23] implemented nonlinear impedance parameters on transfemoral prostheses, they did not enforce continuity. Moreover, the impedance functions in these studies depended on the vertical reaction force measured using an onboard load cell, thereby increasing the weight and cost of the prosthesis. Finally, these

studies did not present a tuning regime for the proposed impedance controllers making implementation difficult.

Few studies enforced continuity of impedance parameters. The study in [24] derived polynomials as a function of gait progression (0%-100%) for ankle stiffness and damping using a least squares fit. These impedance parameters were tested on a transfemoral prosthesis for level walking. Since these polynomials were a function of gait progression alone, this control scheme did not rely on vertical reaction force like [18], [22], [23]. Further, this control scheme had fewer tuning parameters than [15]–[17], [25], while also emulating the continuous nonlinear nature of true human joint impedances [19]–[21].

C. Objectives and contributions of this study

This study extends work presented in [24] to estimating ankle and knee impedance parameters for sloped walking. While the ankle will be controlled purely using impedance control with a finite state machine, the knee will be controlled using a hybrid controller similar to the work [11]. Thus, the knee impedance estimation will be limited to the stance phase. This paper limits its scope to discrete equilibria, but future work will investigate a continuum of equilibria. The proposed impedance control will have fewer tuning parameters than the state-of-the-art and will not rely on an onboard load cell, thereby reducing the cost of the overall prosthesis.

Principal Component Analysis (PCA) is used to reduce the dimensionality of impedance parameters. The authors in [9] extracted basis functions that spanned ankle and knee kinematics. This shows that sloped walking gait kinematics and kinetics obey certain trends. Thus, similar trends are hypothesized for impedance parameters. The resulting trends will serve as the foundation for a tuning regime. Both the estimated impedance parameters and the tuning regime will be tested in an emulated prosthesis study on varying slopes: -10° , -5° , $+5^\circ$, and $+10^\circ$. The contributions of this paper are: (i) set of stiffness and damping basis functions for impedance control of a transfemoral prosthesis on sloped terrain, (ii) a tuning regime for said impedance functions.

II. PROPOSED CONTROL FRAMEWORK

The ankle is controlled using an impedance controller. Since the ankle remains dorsiflexed during swing, a single swing equilibrium angle suffices for control. The knee however is more animated during swing. A poorly timed knee extension can lead to impact, which can result in the user stumbling. Impedance control strategies with discrete equilibria can result in such a mistiming. Contrarily, trajectory tracking ensures smoothness. Thus, a hybrid knee control strategy consisting of impedance control and trajectory tracking is utilized in this study, detailed in [11]. B-spline polynomials ensure a smooth transition from impedance control to trajectory tracking. As noted in Section I, the gait sectioning for impedance control must vary with the slope's angle. A gait cycle is characterized by a heel-strike to another heel-strike on the same limb. All measurements therein are

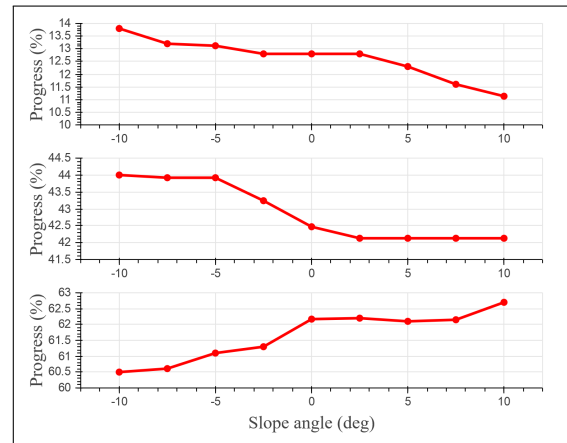


Fig. 1. The variation in the stages of the gait cycle as a function of the slope's angle. **Top:** Flat-foot, **Middle:** Heel-off, **Bottom:** Toe-off.

mapped to 0%-100% regardless of the walking speed and slope. In this study the gait is sectioned into 4 phases : heel-strike ($\phi_{HS} \equiv 0\%$) to flat-foot (ϕ_{FF}), flat-foot (ϕ_{FF}) to heel-off (ϕ_{HO}), heel-off (ϕ_{HO}) to toe-off (ϕ_{TO}), and toe-off (ϕ_{TO}) to the end of the gait cycle (100%).

An analysis of the sloped walking data in [26] revealed that the instants at which ϕ_{FF} , ϕ_{HO} , and ϕ_{TO} occur varies with the slope's angle. Fig. 1 provides an estimate of when each stage of the gait cycle occurs during sloped walking. The values shown in Fig. 1 were used to define the phases of the finite state machine.

In this study, a control scheme is considered successful if it can emulate healthy human gait [15], [18], [23]. Specifically: (i) the ankle has more dorsiflexion pre- and post-heel-strike during upslope walking, (ii) lesser push-off power and higher damping post heel-strike during downslope walking, (iii) more push-off power during upslope walking, and (iv) the knee is more flexed during early and midstance of downslope walking [26].

III. IMPEDANCE ESTIMATES FOR IMPEDANCE CONTROL OF A TRANSFEMORAL PROSTHESIS

For human-like walking, the torque produced by the impedance controller should be similar to that of healthy human walking, say τ_{data} . This study used the sloped walking data reported in [26] for τ_{data} , θ , and $\dot{\theta}$. Note that the latter two are replaced by real-time angle and velocity feedback during testing. The least squares method thus minimizes the norm of the difference between τ in (1) and τ_{data} . Since the knee is controlled via impedance control only during stance phase, the knee's impedance estimation (and thereby cost function) was limited to the stance phase.

Perturbation studies have shown impedance parameters to vary nonlinearly during the stance phase and have little to no variation during the swing phase [20], [21]. To capture the impedance nonlinearities (during stance), K and D were represented by polynomial functions of gait progression. The orders of the polynomials were adjusted to get a better fit while avoiding over-fitting. The impedance parameters were

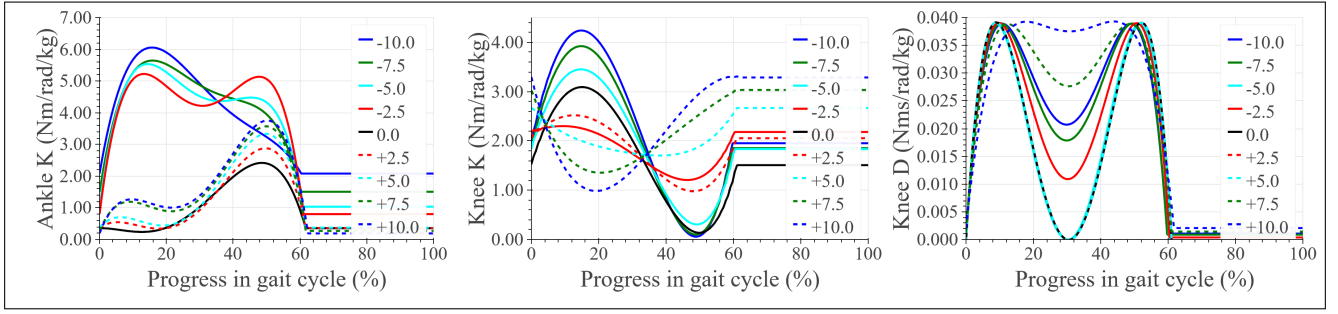


Fig. 2. **Left:** Estimated ankle stiffness across all slopes, **Middle:** Estimated knee stiffness across all slopes, and **Right:** Estimated knee damping across all slopes.

assigned constant values during the swing phase. Supposing m and n represent the order of the K and D polynomials respectively, the impedance parameters at instant $t \in [0, 1]$ can be computed as follows (note that $t = 0$ signifies heel-strike, while $t = 1$ is the end of the gait cycle),

$$K(t) = \begin{cases} \sum_{i=0}^m k_i t^i & \text{for } 0 \leq t < \phi_{TO} \\ k_0 & \text{for } \phi_{TO} \leq t \leq 1 \end{cases} \quad (2)$$

$$D(t) = \begin{cases} \sum_{i=0}^n d_i t^i & \text{for } 0 \leq t < \phi_{TO} \\ d_0 & \text{for } \phi_{TO} \leq t \leq 1 \end{cases} \quad (3)$$

The terms k_i and d_i represent the coefficients of the stiffness and damping polynomials, respectively. The stiffness and damping parameters during swing were assigned the values k_0 and d_0 . This enforced continuity of the impedance parameters from one gait cycle to another (i.e. $K(0) = K(1)$ and $D(0) = D(1)$). Presented below is the optimization problem,

$$\min_{\theta_{eq}, k_i, d_i} \|\tau_{data} - \tau\|_2 \quad (4)$$

$$\text{Subject to: } K(t) \geq 0 \quad D(t) \geq 0 \quad (5)$$

$$\text{Continuity of } K \text{ and } D \text{ at } t = \phi_{TO} \quad (6)$$

$$|\theta_{eq}| \leq c_1 \quad (7)$$

$$|\Delta\tau/\Delta t| \leq c_2 \quad (8)$$

Note that θ_{eq} represents a set of equilibrium angles, one for each stage of the finite state machine. The positivity of K and D is ensured with the constraints listed in (5). The constraint (6) assures continuity of the impedance functions during the stance to swing transition. The scalar, c_1 , is a bound on the equilibrium angles. $c_1 = 16^\circ$ for the ankle and $c_1 = 36^\circ$ for the knee. Further, the constraint (8) forces the resulting τ to be continuous using a Lipschitz constant, c_2 . Additional bounds were added, as needed, to restrict the value of the damping parameters. The optimization problem was solved using Scipy's minimization function.

A. Optimization results

Fig. 2 presents the estimated stiffness and damping functions for the ankle and knee. All stiffness and damping polynomials were found to be of order 4. Per the hypothesis, ankle stiffness, knee stiffness, and knee damping displayed trends across varying slope angles. As the slope angle varied from -10° to 0° , the joint stiffness (of both ankle and knee)

were found to decrease post-heel-strike. The high stiffness helps counter the high heel-strike impact experienced during downslope walking. Further, since the amount of push-off assistance decreases with the slope descent angle, it is reasonable to expect lower stiffness at heel-off. On the contrary, as the slope angle increases from 0° to 10° , the required push-off torque increases, thus mandating higher joint stiffness. More importantly, the trend of the ankle stiffness function at level walking matches that of perturbation studies [19], [20]. Although ankle damping parameters were estimated, they did not follow trends as consistent as the ones portrayed by stiffness. Knee damping, on the other hand, was found to be high during mid-stance at steeper slopes (-10.0° , -7.5° , $+7.5^\circ$, 10.0°). At less steep slopes (-5.0° to $+5.0^\circ$), knee damping was relatively the same. Knee stiffness and knee damping at -2.5° were found to break the trends seen in Fig. 2. On closer observation of the joint torques reported in [26], a similar anomaly was observed in both knee and ankle joint torques. To the authors' knowledge, the contributors of the data set in [26] have not addressed this anomaly.

Some of the equilibrium angles have been presented in Table I. The ankle's equilibrium angles depicted a trend consistent with the ankle equilibrium angles reported in perturbation studies [21]. The degree of variation seen among these equilibrium angles appear to decrease as the downslope angle became steeper. The opposite behavior was seen in the ankle's equilibrium angles for upslope walking. The knee's equilibrium angles were generally more flexed on steep slopes, enabling terrain adaption during upslope walking and

TABLE I
ANKLE AND KNEE EQUILIBRIUM ANGLES.

Slope	Ankle Equilibrium Angles (deg)			
	Phase 1	Phase 2	Phase 3	Phase 4
-10.0°	-0.03	-3.94	-5.56	3.58
0°	5.60	-11.06	-16.00	0.84
$+10.0^\circ$	7.19	-15.0	-16.00	6.37
Slope	Knee Equilibrium Angles (deg)			
	Phase 1	Phase 2	Phase 3	
-10.0°	8.90	10.36	30.00	
0°	10.26	5.83	13.86	
$+10.0^\circ$	36.00	24.61	20.00	

shock absorption during downslope walking. The trends in the ankle's and knee's equilibrium angles are fairly similar to those used in prior studies on impedance control [15], [17].

B. Principal component analysis

The set of nine stiffness and damping functions were reduced in dimension to two using Principal Component Analysis (PCA). The resulting basis functions account for more than 95% of the information have been presented in Fig. 3 with their weights. Since the ankle damping estimates did not follow any trend, the depicted weights are those used during experimental trials (detailed in the following section). Interestingly, the weights for ankle and knee stiffness basis functions were found to obey nearly linear trends within upslope and downslope walking. As noted earlier, the weights for -2.5° did not obey this linear trend. Ignoring -2.5° , the weights for knee damping varied monotonically between -10.0° to -5.0° and $+5.0^\circ$, 10.0° , and remained fairly constant between -5.0° to $+5.0^\circ$. These monotonic variations are in agreement with the hypothesis that impedance estimates should obey trends during sloped walking. Given these trends, one can design a sloped walking impedance controller for any slope, making the proposed controller easy to implement.

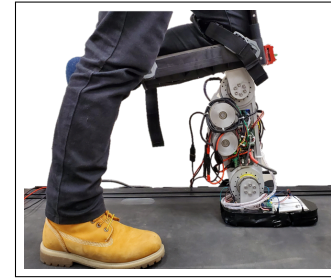


Fig. 4. Subject with an L-shaped emulator and the prosthesis AMPRO II.

IV. EXPERIMENT

The estimated impedance parameters were tested on a powered transfemoral prosthesis, AMPRO II (shown in Fig. 4). AMPRO II is operated by a micro-processor (element14, BeagleBone Black) that controls an actuated ankle and knee joint. The progress in the gait cycle was identified using a parameter that linearly increases from 0 to 1 as the gait progresses from 0% to 100%. This is termed as a time-based scheme. A force sensor (Tekscan, FlexiForce A502) placed under the heel was used to initialize the parameter to 0. Many studies have implemented state-based schemes, wherein a state (also known as phase variable) such as the thigh angle is used to identify the progress of the gait cycle [11], [27]. For successful implementation, the phase variable should vary monotonically as the gait progresses [28]. Unfortunately, current phase variables are known to be inaccurate at lower walking speeds [11], [27]. This study is aimed at evaluating the performance of the estimated impedance parameters. Thus, it was preferred the performance be unaffected by the possible inaccuracies of state-based schemes.

A. Experimental protocol

An indoor experiment was conducted with a healthy young subject (male, 170cm, 70kg weight). The subject used an L-shape simulator to emulate an amputee's gait. The subject was asked to walk on a treadmill set to a fixed speed of 0.7m/s. A low speed was selected to avoid fatigue at steeper slopes. Further, a fixed speed facilitates a controlled comparison across different slopes. The controller was also tested at a speed of 1m/s on level ground to demonstrate the feasibility of the proposed controller at different walking speeds. The safety of the participant was assured with handrails located on either side of the treadmill. The experiment protocol has been approved by the Institutional Review Board (IRB) at Texas A&M University (IRB2015-0607F). The treadmill was angled at -10° , -5° , $+5^\circ$, and $+10^\circ$ using scissor jacks.

B. Tuning

Given the slope's angle, an initial guess for joint stiffness and damping can be found using the impedance basis functions and their weights. The resulting stiffness and damping functions can be tuned further to generate the desired gait kinematics and kinetics. Prior tuning, both impedance functions should be multiplied by the subject's body mass. This

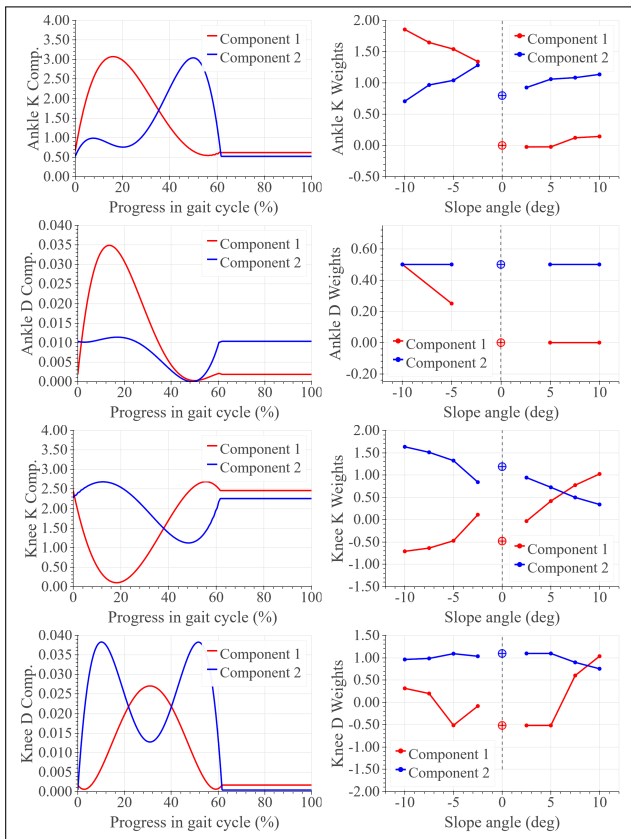


Fig. 3. **LEFT:** Basis functions (a.k.a components) for ankle and knee stiffness and damping in Nm/rad/kg and Nms/rad/kg respectively. The term Comp. refers to Component. **RIGHT:** The weights for the components at different slope angles.

study proposes tuning the impedance functions as follows.

$$K_{tuned}(t) = \alpha K(t) + \gamma \quad (9)$$

$$D_{tuned}(t) = \beta D(t) \quad (10)$$

where α and β are scaling factors, and γ is an offset. Each joint has its own scaling and offset terms. This study recommends tuning the controller for level, -10° , and $+10^\circ$ slope, followed by linearly interpolating parameters for other slope angles.

The factor α affects the amount of resistance provided by the system to ankle dorsiflexion and knee flexion. With the ankle, lowering α reduces push-off assistance, while with the knee, lowering α challenges the stability of a flexed knee. The recommended approach is to decrease α until the desired ankle dorsiflexion and knee flexion is observed in Phase 2. This study targeted 4° of ankle dorsiflexion and 10° of knee flexion. According to the participant's preference, increase or decrease push-off assistance by respectively increasing or decreasing the ankle's plantarflexed equilibrium angle during Phase 3. Tune β to reach a compromise between the amount of damping preferred by the participant at heel-strike and smooth terrain adaptation post heel-strike. Increase the offset γ to counter gravity and maintain ankle dorsiflexion during swing and knee flexion during terminal stance. All equilibrium angles should be tuned to respect the actuator's acceleration limits while following the trends shown in Table I and discussed in Section III-A.

V. RESULTS AND DISCUSSION

The final set of tuned equilibrium angles has been presented in Table II. As stated earlier, the equilibrium angles for -5° and $+5^\circ$ were found through linear interpolation. For all sloped conditions: $\beta = 0.5$ for both knee and ankle, $\gamma = 20$ for the ankle, and $\gamma = 50$ for the knee. The high scaling and offset factors compensate for the high inherent friction at the joints and high inertia. The results that follow account for 10 consecutive gait cycles with the prosthesis.

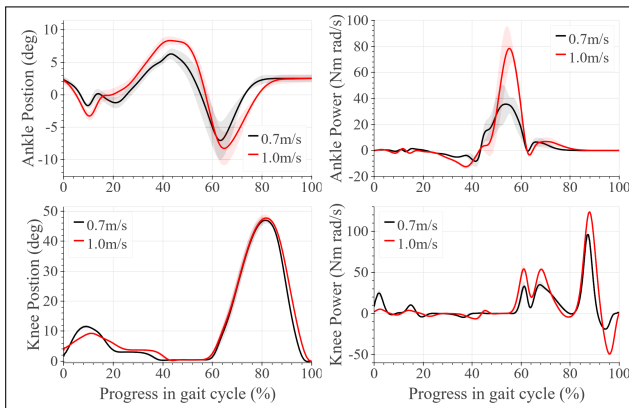


Fig. 5. Ankle and Knee position and power at 0.7m/s and 1m/s level walking. While the solid line indicates the average over 10 consecutive gait cycles, the shaded region represents one standard deviation.

TABLE II
TUNED ANKLE AND KNEE EQUILIBRIUM ANGLES.

Slope	Ankle Equilibrium Angles (deg)			
	Phase 1	Phase 2	Phase 3	Phase 4
-10.0°	0.0	-2.51	-7.49	0.0
0°	0.0	-5.01	-14.99	5.00
$+10.0^\circ$	5.01	-5.01	-14.99	5.00
Slope	Knee Equilibrium Angles (deg)			
	Phase 1	Phase 2	Phase 3	
-10.0°	10.12	18.0	18.0	
0°	10.26	5.83	13.86	
$+10.0^\circ$	11.97	10.25	14.99	

A. Level walking

For level walking, neither the knee's nor the ankle's stiffness functions were scaled (i.e. $\alpha = 1$). Both joint kinematics and kinetics, at $0.7m/s$ and $1.0m/s$, have been presented in Fig. 5. The impedance parameters for both level walking tests were the same. Both kinematics and kinetics resemble healthy human walking [29]. Specifically, more ankle dorsiflexion during midstance and push-off assistance was observed at the higher walking speed. The peak power was found to increase by factor of 2.2 with the walking speed, thus, proving the feasibility of the proposed control scheme for variable walking speeds.

B. Downslope walking

The ankle and knee stiffnesses were scaled down by $\alpha = 0.67$ and $\alpha = 0.5$ respectively for downslope walking. The top two rows in Fig. 6 presents the joint position, torque, and power for level and downslope walking. The following are the key observations as the slope grew steeper: (i) increased ankle plantarflexion upon heel-strike as a result of the foot adapting to the sloped terrain, (ii) reduced ankle plantarflexion at toe-off, (iii) reduced ankle dorsiflexion during swing, (iv) increased damping effect in the torque curves upon heel-strike, (v) reduced ankle push-off torque and peak power (by a factor of 0.54 and 0.75 at -5° and -10° respectively), (vi) more knee flexion during midstance, (vii) lesser flexive knee torque during midstance. All of these trends resemble healthy human walking [7], [26]. The heel-off plantarflexion appears earlier at -5° , leading to an earlier push-off power peak when compared to level walking and -10° . This is likely an artifact of the time-based scheme and can be corrected with an accurate state-based scheme.

C. Upslope walking

The bottom two rows in Fig. 6 shows the joint position, torque, and power for level, and upslope walking. Neither the ankle's nor the knee's stiffness functions were scaled down. The following are the key observations as the slope grew steeper: (i) increased ankle dorsiflexion upon heel-strike for terrain adaptation, (ii) more ankle plantarflexion at toe-off, (iii) higher ankle dorsiflexion during swing phase, (iv) increased ankle push-off torque and peak power (by a factor of 1.45 and 1.56 at $+5^\circ$ and $+10^\circ$ respectively), (v) more

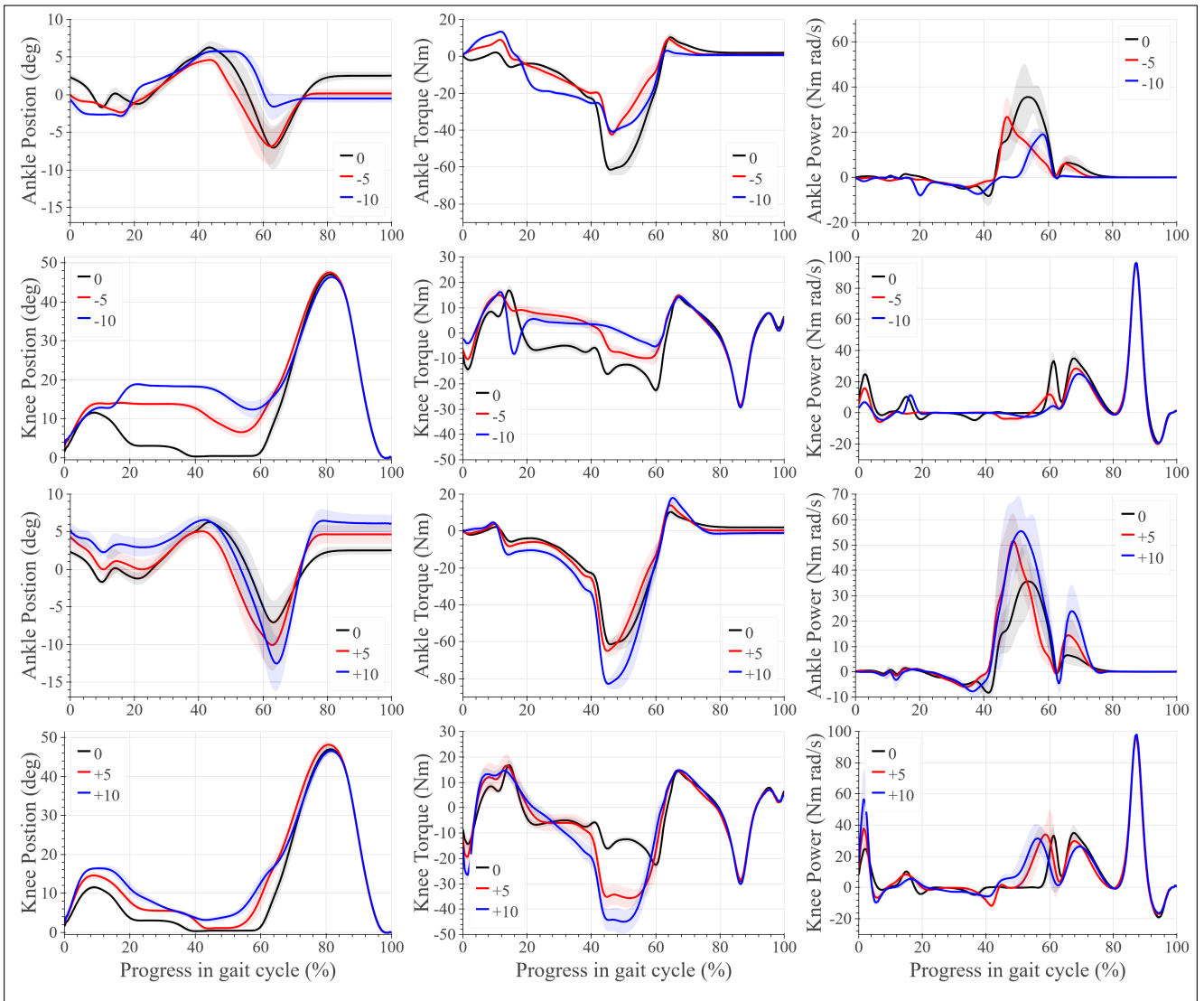


Fig. 6. **Left:** Joint angle, **Middle:** Joint torque, and **Right:** Joint power. While the solid lines indicate the average over 10 consecutive gait cycles, the shaded regions represent one standard deviation

flexing knee torque during midstance. Again, all of these trends are consistent with those observed in healthy human walking trials [7], [26].

VI. CONCLUSION

This study proposed an impedance control strategy for sloped walking using continuous stiffness and damping functions estimated via optimization. Unlike impedance controllers found in literature, the proposed impedance functions maintain continuity across the gait cycle and are not functions of the vertical ground reaction force, eliminating the need for an expensive load cell. The resulting impedance functions were found to obey monotonic trends across slope angles. Principal component analysis of the estimated impedance functions revealed two basis impedance (stiffness and damping) functions for both the ankle and the knee. The weights of these basis functions were also found to obey monotonic trends across the slopes. These trends serve as a guide for designing impedance controllers for any slope

angle. The resulting impedance functions can be easily tuned by observing key gait characteristics such as desired ankle dorsiflexion, knee flexion during midstance, and push-off assistance. Unlike the state-of-the-art impedance controllers, the proposed scheme only has 7-8 tuning parameters per joint, making tuning significantly easier. Experiments with a transfemoral prosthesis demonstrated the feasibility of the proposed scheme for sloped walking. Some notable observations were high push-off assistance during upslope walking and the opposite during downslope walking. High damping at heel-strike was observed during downslope walking.

Tests with amputees will further attest to the controller's performance. Metrics such as gait symmetry will be used and the likeliness of the generated gait to healthy walking will be quantified. Future work will include implementing an accurate state-based scheme for sloped walking, replacing the current discrete equilibrium angles with a continuum of equilibria.

REFERENCES

- [1] K. Ziegler-Graham, E. J. MacKenzie, P. L. Ephraim, T. G. Travison, and R. Brookmeyer, "Estimating the prevalence of limb loss in the united states: 2005 to 2050," *Archives of Physical Medicine and Rehabilitation*, vol. 89, no. 3, pp. 422 – 429, 2008.
- [2] L. Kraus, "2016 Disability Statistics Annual Report," University of New Hampshire, Durham, Tech. Rep., 2017.
- [3] A. H. Peirano and R. W. Franz, "Spirituality and quality of life in limb amputees," *The International journal of angiology: official publication of the International College of Angiology, Inc*, vol. 21, no. 1, p. 47, 2012.
- [4] M. Goldfarb, "Consideration of powered prosthetic components as they relate to microprocessor knee systems," *JPO: Journal of Prosthetics and Orthotics*, vol. 25, no. 4S, pp. P65–P75, 2013.
- [5] H. M. Herr and A. M. Grabowski, "Bionic ankle-foot prosthesis normalizes walking gait for persons with leg amputation," *Proceedings of the Royal Society B: Biological Sciences*, vol. 279, no. 1728, pp. 457–464, 2012.
- [6] A. S. McIntosh, K. T. Beatty, L. N. Dwan, and D. R. Vickers, "Gait dynamics on an inclined walkway," *Journal of Biomechanics*, vol. 39, no. 13, pp. 2491–2502, 2006.
- [7] A. N. Lay, C. J. Hass, and R. J. Gregor, "The effects of sloped surfaces on locomotion: A kinematic and kinetic analysis," *Journal of Biomechanics*, vol. 39, no. 9, pp. 1621 – 1628, 2006.
- [8] A. Vrieling, H. van Keeken, T. Schoppen, E. Otten, J. Halbertsma, A. Hof, and K. Postema, "Uphill and downhill walking in unilateral lower limb amputees," *Gait & Posture*, vol. 28, no. 2, pp. 235–242, Aug 2008.
- [9] K. R. Embry, D. J. Villarreal, R. L. Macaluso, and R. D. Gregg, "Modeling the kinematics of human locomotion over continuously varying speeds and inclines," *IEEE Transactions on Neural Systems and Rehabilitation Engineering*, vol. 26, no. 12, pp. 2342–2350, Dec 2018.
- [10] W. Hong, K. Chao, and P. Hur, "The effect of inclination and walking speed on foot placement for slope walking," in *2019 American Society of Biomechanics/International Society of Biomechanics (ASB/ISB)*, Aug 2019.
- [11] W. Hong, V. Paredes, K. Chao, S. Patrick, and P. Hur, "Consolidated control framework to control a powered transfemoral prosthesis over inclined terrain conditions," in *2019 International Conference on Robotics and Automation (ICRA)*, May 2019, pp. 2838–2844.
- [12] V. Paredes, W. Hong, S. Patrick, and P. Hur, "Upslope walking with transfemoral prosthesis using optimization based spline generation," in *2016 IEEE/RSJ International Conference on Intelligent Robots and Systems (IROS)*, Oct 2016, pp. 3204–3211.
- [13] D. Quintero, D. J. Villarreal, D. J. Lambert, S. Kapp, and R. D. Gregg, "Continuous-phase control of a powered knee–ankle prosthesis: Amputee experiments across speeds and inclines," *IEEE Transactions on Robotics*, vol. 34, no. 3, pp. 686–701, June 2018.
- [14] B. E. Lawson, J. Mitchell, D. Truex, A. Shultz, E. Ledoux, and M. Goldfarb, "A Robotic Leg Prosthesis: Design, Control, and Implementation," *IEEE Robotics & Automation Magazine*, vol. 21, no. 4, pp. 70–81, 2014.
- [15] F. Sup, H. A. Varol, and M. Goldfarb, "Upslope Walking With a Powered Knee and Ankle Prosthesis: Initial Results With an Amputee Subject," *IEEE Transactions on Neural Systems and Rehabilitation Engineering*, vol. 19, no. 1, pp. 71–78, Feb 2011.
- [16] D. Wang, M. Liu, F. Zhang, and H. Huang, "Design of an expert system to automatically calibrate impedance control for powered knee prostheses," in *2013 IEEE 13th International Conference on Rehabilitation Robotics (ICORR)*, 2013, pp. 1–5.
- [17] Y. Wen, J. Si, A. Brandt, X. Gao, and H. H. Huang, "Online reinforcement learning control for the personalization of a robotic knee prosthesis," *IEEE Transactions on Cybernetics*, vol. 50, no. 6, pp. 2346–2356, 2020.
- [18] N. P. Fey, A. M. Simon, A. J. Young, and L. J. Hargrove, "Controlling knee swing initiation and ankle plantarflexion with an active prosthesis on level and inclined surfaces at variable walking speeds," *IEEE Journal of Translational Engineering in Health and Medicine*, vol. 2, pp. 1–12, 2014.
- [19] E. J. Rouse, R. D. Gregg, L. J. Hargrove, and J. W. Sensinger, "The Difference Between Stiffness and Quasi-Stiffness in the Context of Biomechanical Modeling," *IEEE Transactions on Biomedical Engineering*, vol. 60, no. 2, pp. 562–568, Feb 2013.
- [20] E. J. Rouse, L. J. Hargrove, E. J. Perreault, and T. A. Kuiken, "Estimation of Human Ankle Impedance During the Stance Phase of Walking," *IEEE Transactions on Neural Systems and Rehabilitation Engineering*, vol. 22, no. 4, pp. 870–878, 2014.
- [21] H. Lee, E. J. Rouse, and H. I. Krebs, "Summary of Human Ankle Mechanical Impedance During Walking," *IEEE Journal of Translational Engineering in Health and Medicine*, vol. 4, pp. 1–7, 2016.
- [22] A. M. Simon, K. A. Ingraham, N. P. Fey, S. B. Finucane, R. D. Lipschutz, A. J. Young, and L. J. Hargrove, "Configuring a powered knee and ankle prosthesis for transfemoral amputees within five specific ambulation modes," *PLOS ONE*, vol. 9, no. 6, pp. 1–10, 06 2014.
- [23] K. Bhakta, J. Camargo, P. Kunapuli, L. Childers, and A. Young, "Impedance Control Strategies for Enhancing Sloped and Level Walking Capabilities for Individuals with Transfemoral Amputation Using a Powered Multi-Joint Prosthesis," *Military Medicine*, vol. 185, pp. 490–499, 12 2019.
- [24] N. Anil Kumar, W. Hong, and P. Hur, "Impedance control of a transfemoral prosthesis using continuously varying ankle impedances and multiple equilibria," in *2020 IEEE International Conference on Robotics and Automation (ICRA)*, 2020, pp. 1755–1761.
- [25] F. Sup, A. Bohara, and M. Goldfarb, "Design and control of a powered transfemoral prosthesis," *The International Journal of Robotics Research*, vol. 27, no. 2, pp. 263–273, 2008.
- [26] K. Embry, D. Villarreal, R. Macaluso, and R. Gregg, "The effect of walking incline and speed on human leg kinematics, kinetics, and emg," 2018. [Online]. Available: <http://dx.doi.org/10.21227/gk32-e868>
- [27] S. Rezazadeh, D. Quintero, N. Divekar, and R. D. Gregg, "A phase variable approach to volitional control of powered knee-ankle prostheses," in *2018 IEEE/RSJ International Conference on Intelligent Robots and Systems (IROS)*, Oct 2018, pp. 2292–2298.
- [28] D. J. Villarreal and R. D. Gregg, "Unified phase variables of relative degree two for human locomotion," in *Engineering in Medicine and Biology Society (EMBC), 2016 IEEE 38th Annual International Conference of the*. IEEE, 2016, pp. 6262–6267.
- [29] D. A. Winter, *Biomechanics and motor control of human movement*, 4th ed. Wiley, 2009.